Statistical-acoustics models of energy decay in systems of coupled rooms and their relation to geometrical acoustics[a)]

Jason E. Summers,[b),c)] Rendell R. Torres, and Yasushi Shimizu[d)]
Program in Architectural Acoustics, Rensselaer Polytechnic Institute, Troy, NY 12180

(Received 26 August 2003; revised 19 March 2004; accepted 2 May 2004)

An improved statistical-acoustics model of high-frequency sound fields in coupled rooms is developed by incorporating into prior models geometrical-acoustics corrections for both energy decay within subrooms and energy transfer between subrooms. The conditions under which statistical-acoustics models of coupled rooms are valid approximations to geometrical acoustics are examined by comparison of computational geometrical-acoustics predictions of decay curves in two- and three-room systems with those of both improved and prior statistical-acoustics models. The accuracy of the decay model used within subrooms is found to have a primary influence on the accuracy of predictions in coupled systems. Likewise, nondiffuse transfer of energy is shown to significantly affect decay of energy in systems of coupled rooms. The decrease in energy density of the reverberant field with distance from the source, which is predicted by geometrical acoustics, is found to result in spatial dependence of decay-curve shape for certain coupling geometries. Geometrical effects are shown to contribute to the failure of statistical-acoustics models in the case of strong coupling between subrooms; thus, previously proposed statistical-acoustics criteria cannot predict the point at which the models break down with consistent accuracy. [DOI: 10.1121/1.1763974]

PACS numbers: 43.55.Br, 43.55.Ka [MK] Pages: 958–969

I. INTRODUCTION

The high-frequency modeling techniques of statistical acoustics (SA) and geometrical acoustics (GA) are increasingly being applied to systems of large, coupled rooms as the use of auxiliary coupled volumes in the design of performance spaces becomes more frequent. SA models offer the advantages of speed and simplicity, but their accuracy in predicting the sound fields in systems of large, coupled rooms has not been established. The interrelationship of these two modeling techniques has been theoretically characterized[1–3] and studied in single-volume rooms both computationally[4–6] and experimentally.[7] Based on GA concepts, semiempirical refinements of Sabine's original SA model[8] have been developed.[9–12] In systems of coupled rooms SA models involve additional assumptions that further limit their agreement with GA models. Thus, the relationships established between SA and GA for single-volume rooms must be reevaluated for systems of coupled rooms. Many of the semiempirical corrections developed for SA models of single-volume rooms have not been applied to SA models of coupled rooms. Moreover, new corrections can be developed to address the additional assumptions required to model coupled rooms. This paper describes an improved SA model of coupled rooms, which comprises prior models while incorporating additional corrections, and examines the relationship of SA models to GA.

An SA model of two coupled rooms was first developed by Davis[13] based on a system of coupled ordinary differential equations (ODEs). Detailed expositions of this model have been given by Cremer and Müller[14] and Lyle.[15,16] Kuttruff[17] has generalized this model to systems of an arbitrary number of coupled rooms by expressing it in matrix formalism (though Peutz[18] earlier used an analog computer to solve the same system of ODEs). Eyring[19] modified Davis's derivation to incorporate an alternative decay model.[9]

II. STATISTICAL-ACOUSTICS MODEL

A. Models of single-volume rooms

The Sabine model[8] is a limiting case of GA in enclosures that are ergodic, sufficiently mixing, and weakly absorbing.[1,3] In conditions for which the assumptions of the Sabine model are not valid, additional information is required in order to yield a true first-order correction to the Sabine model.[20] Other decay models[9–11] can often, but not always, yield predictions that are more accurate than those of the Sabine model.[2] The Eyring model[9] considers only the first moment of the free-path distribution, and thus assumes energy is lost every time a phonon travels a distance of one mean-free path $\langle \bar{\ell} \rangle$. Defining η as the ratio of the Eyring absorption exponent α' to the geometrically averaged absorption coefficient $\bar{\alpha}$

$$\eta = \frac{\alpha'}{\bar{\alpha}}, \tag{1}$$

allows the Eyring decay constant δ' to be expressed in terms of the Sabine decay constant

[a)]Portions of this work have been presented at the 143rd meeting of the Acoustical Society of America [J. Acoust. Soc. Am. **111**, 2390 (A) (2002)].
[b)]Electronic mail: summers@abyss.nrl.navy.mil
[c)]Current address: Naval Research Laboratory, Washington, D.C. 20375-5350.
[d)]Current address: Yamaha Corporation, 10-1 Nakazawa-cho, Hamamatsu 430-8650 Japan.

$$\delta' = \frac{cS\alpha'}{8V} = \eta\delta, \tag{2}$$

where c is the speed of sound, S is the total surface area, and V is the volume of the room. Regardless of its merit in single-volume rooms, the similar Millington–Sette model[10] is not suitable for use in coupled rooms because it predicts that any surface with $\alpha=1$, such as a coupling aperture, causes decay rate to become infinite.[17]

Kuttruff[11] showed that accounting for the second moment of the free-path distribution leads to the absorption exponent

$$\alpha'' = -\ln(1-\overline{\alpha})\left[1+\frac{\gamma^2}{2}\ln(1-\overline{\alpha})\right], \tag{3}$$

where γ^2 is the normalized variance $(\langle\overline{\ell^2}\rangle-\langle\overline{\ell}\rangle^2)/\langle\overline{\ell}\rangle^2$. The decay constant δ'' can be expressed by defining η as before.

In the presence of strong nonuniform absorption the Sabine model fails. But, under these conditions, a room that is sufficiently mixing can decay exponentially.[7,21,22] The decay rate, however, may not be well predicted by SA models.[17] Embleton[12] has presented a Markov-process implementation of the radiosity method that specifically accounts for this effect. The model reduces to a simple form in the practical case of a room having only two distinct types of surface. Given an absorbent floor or aperture area S_1 with absorption coefficient α_1 and the remaining area S_0 having a uniform absorption coefficient α_0, the absorption exponent α''' is given by

$$\alpha''' = -\ln[1-(\overline{\alpha}+\Delta\overline{\alpha})], \tag{4}$$

where

$$\Delta\overline{\alpha} = \frac{(\alpha_1-\alpha_2)^2}{1-\overline{\alpha}}\left(\frac{S_1}{S}\right)^2. \tag{5}$$

As previously developed, this model only accounts for the mean of the free-path distribution. If the variance in the free-path distribution is addressed the absorption exponent is given by

$$\alpha'''' = -\ln[1-(\overline{\alpha}+\Delta\overline{\alpha})]\left\{1+\frac{\gamma^2}{2}\ln[1-(\overline{\alpha}+\Delta\overline{\alpha})]\right\}. \tag{6}$$

The resulting new decay model is here termed the Kuttruff–Embleton model. The correction term $\Delta\overline{\alpha}$ is positive; thus these models predict larger decay constants than the unmodified Eyring or Kuttruff expressions, respectively. This is correct only for some enclosure geometries. For example, predictions agree with GA in rectangular parallelepipeds with one absorptive surface only if the absorptive surface is one of the larger surfaces.[17] Further, if more than two types of surface exist in a room, applying the simplified form of these models can lead to substantial error.[12]

Propagation loss can be accounted for in any of the models discussed above by adding a factor of $4mV$ to the total absorption power, where m is the energy dissipation coefficient of air expressed in units of Nepers per meter.[23]

In coupled rooms the shapes of decay curves are functions of both decay constants and steady-state energy densities. For this reason, it is especially important that a SA model predict both behaviors accurately. The expression for steady-state energy density ε_0 in a single-volume room containing a source of power Π,

$$\varepsilon_0 = \frac{4\Pi\exp(-A/S)}{cA}, \tag{7}$$

proposed by Vorländer,[24] was found most accurate when compared to GA predictions. The total absorption power A is defined as the product of the surface area and the average absorption coefficient or absorption exponent. The Sabine form, $A=S\overline{\alpha}$, has been adopted for this work. While this model predicts a uniform level of the reverberant field, it is known[25,26] that the steady-state level of the reverberant sound decreases with distance from the source. If it is assumed that the energy density due to the reverberant field decays exponentially and the instantaneous level of the reverberant field is uniform throughout the space, ε_0 will be given by the sum of the energy density contributed by the direct sound and the integration of the reverberant field energy density arriving after the direct sound. Assuming spherical propagation from the source and a receiver located at a distance r from the source, the expression for energy density is[26]

$$\varepsilon_0(r) = \frac{\Pi}{4\pi r^2 c} + \varepsilon_0\exp\left(-2\delta\frac{r}{c}\right). \tag{8}$$

B. Prior models of coupled rooms

When two or more rooms are joined together in such a way that energy can be transmitted between them, the rooms constitute a coupled system. The reverberant field in a system of coupled rooms is not described by SA models that have been developed for single-volume rooms.

Knudsen[23] has suggested that, for a uniform distribution of absorption between the subrooms, single-slope decay curves will result that can be described by the Eyring model using the mean-free path of the total system $\langle\overline{\ell}\rangle$

$$\varepsilon(t) = \varepsilon_0\exp\left(\frac{-c}{\langle\overline{\ell}\rangle}\alpha'\right). \tag{9}$$

This expression can be refined by replacing α' with another absorption exponent [e.g., Eqs. (3), (4), or (6)]. In rooms of disparate size the conjecture is incorrect because the bimodality of the free-path distribution is pronounced and double-slope decay curves result.[27] But, even if the decay curves in the subrooms are dominated by a single rate, it may be inaccurate to treat the subrooms as a single room.[16]

To treat a more general case, an enclosure consisting of coupled rooms must be modeled as a system of independently decaying subrooms that interact through the exchange of energy between their diffuse fields. The expression of this by Kuttruff[17] is formally equivalent to all prior models of coupled rooms based on the Sabine model of energy decay within subrooms.

Such dynamic energy-balance approaches assume that (1) each subroom has a unique diffuse sound field and that at coupling aperture(s) there is an abrupt transition between

sound fields, (2) the subrooms of the system interact only by an exchange of diffuse energy, and (3) the decay properties of the subrooms are unaltered by the coupling other than the small shift in the decay constant of each room predicted by the SA model (see, e.g., Ref. 14). The validity of these assumptions is examined in Sec. II D 2.

C. Improved model of coupled rooms

Under the Sabine assumptions irradiation strength $B = \varepsilon c/4$. However, Eyring[19] observed that assuming any decay model other than Sabine's is tantamount to multiplying B by the factor η. Eyring applied this observation only to the case of two coupled rooms with the decay rates in the subrooms predicted by the Eyring decay model. In the improved model presented here, Eyring's observation is used to modify Kuttruff's matrix formulation. Thus, the new model described below can use any of the decay models discussed in Sec. II A—including the newly introduced Kuttruff–Embleton model—to solve for the decay rates in the subrooms of a coupled system containing an arbitrary number of subrooms. If the Sabine model is used within the subrooms $\eta=1$ and the improved model (excluding the additional corrections discussed further below) is identical to Kuttruff's.

The energy density in the ith room is described by

$$\frac{d\varepsilon_i(t)}{dt} = -2\eta_i\zeta_i\varepsilon_i(t) = \frac{\eta_i B_i(t) A_{i0}}{V_i}, \tag{10}$$

where ζ_i is the Sabine decay constant of the ith room when uncoupled, $B_i(t)$ is the irradiation strength in the ith room, and A_{i0} is the absorption power of the ith room exclusive of the coupling area. For a system of N rooms with apertures of area S_{ij} that allow energy to be transferred between the ith and jth rooms, the system of N coupled ODEs representing the dynamic energy balance is, following Kuttruff's derivation[17]

$$\frac{d\varepsilon_i(t)}{dt} = -\eta_i\left(2\zeta_i + \frac{c\sum_{\substack{j=1\\ j\neq i}}^{N} S_{ij}}{4V_i}\right)\varepsilon_i(t) + \sum_{\substack{j=1\\ j\neq i}}^{N} \eta_j \frac{cS_{ij}}{4V_i}\varepsilon_j(t) \quad (i=1...N). \tag{11}$$

The values $B_i(t)$, rather than the decay rates themselves, must be adjusted using the factors η_i to account for different decay models if Eq. (11) is to be self-consistent. Separating the decay terms in the ith room [the first term of the right-hand side of Eq. (11)] into decay due to absorption and decay due to transfer of energy through the aperture(s) essentially separates A_{i0} of Eq. (10) into two terms so that changing the decay rate of the subroom cannot be effected by altering A, since the terms would not add, but rather by altering their common multiplying factor.

Defining a set of constant coefficients ψ_{ij} in the manner of Ref. 17 allows the system to be written in matrix notation

$$\dot{\boldsymbol{\varepsilon}} = \boldsymbol{\Psi}\boldsymbol{\varepsilon} \tag{12}$$

and solved using conventional procedures for such systems of ODEs. The N eigenfunctions of this system are of the form

$$\boldsymbol{\varepsilon}^{(i)} = \boldsymbol{\varepsilon}_0^{(i)} \exp(-2\delta_i t) \quad (i=1...N), \tag{13}$$

with eigenvectors $\boldsymbol{\varepsilon}_0^{(i)}$ and eigenvalues δ_i. The general solution in the ith room is expressed as a linear combination of the eigenfunctions

$$\varepsilon_i(t) = C_1\varepsilon_{i0}^{(1)}\exp(-2\delta_1 t) + \ldots + C_N\varepsilon_{i0}^{(N)}\exp(-2\delta_N t) \quad (i=1...N), \tag{14}$$

where $\varepsilon_{i0}^{(j)}$ is the ith component of the jth eigenvector. By considering the steady-state solution of Eq. (11) the coefficients C_i are solved for in terms of the steady-state energy-density values. These are determined by solving the system of coupled energy-balance equations

$$\frac{\Pi_i}{V_i} = -\sum_{j=1}^{N} \psi_{ij}\varepsilon_j(0) \quad (i=1...N), \tag{15}$$

where Π_i is the power of the source located in the ith room. There is some ambiguity concerning which form of $\boldsymbol{\Psi}$ should be used to solve for steady-state values. Eyring[19] held that his formulation was not appropriate for the steady-state case and should only be used to determine decay rates; instead, the Sabine model should be used for steady-state processes. While use of either can be validated by formal derivation,[17] the Sabine form of $\boldsymbol{\Psi}$ is adopted in this paper. Further, Vorländer's correction is applied to the resulting values of $\varepsilon_j(0)$.

Unlike prior models, this improved model can treat multiple sources distributed throughout the subrooms or sources that simultaneously radiate into more than one subroom. The latter case is accommodated by finding $\Delta\Omega_{ij}$, the fraction of the total solid angle subtended by S_{ij} as viewed from the source (see the appendix A of Ref. 25). For example, given a source of power P located in the ith room of a two-room system two sources are modeled. In the jth room $\Pi_j = P\Delta\Omega_{ij}/4\pi$ and in the ith room $\Pi_i = P - \Pi_j$. For complex aperture configurations, a computational approach must be used. In many cases the ratio $\Delta\Omega_{ij}/4\pi$ can be estimated as the ratio of aperture area to total surface area of the room.

Barron and Lee's revised theory for steady-state energy density[26] explicitly assumes that the reverberant field in a room will decay at a single exponential rate. In a system of N coupled rooms, the reverberant field will, in general, decay as the linear combination of N exponential decays. In this case, the energy contained in the impulse response integrated from the arrival time of the direct sound to infinity summed with the energy density due to the direct sound is given in the ith room by the new expression

$$\varepsilon_0(r) = \frac{\Pi}{4\pi r^2 c} + \sum_{j=1}^{N} C_j\varepsilon_{i0}^{(j)}\exp\left(-2\delta_j\frac{r}{c}\right), \tag{16}$$

where r is the distance from the source to the receiver. It should be noted that r/c is typically much smaller than the reverberation time of the ith room T_i corresponding to δ_i of the subrooms. Therefore, it is the ability of the decay model

to accurately predict the early portion of the decay that is most critical to the accuracy of Eq. (16). Moreover, variation in energy level with position is governed almost entirely by δ_j for which $C_j\varepsilon_{i0}^{(j)}$ is largest, unless the knee of the decay curve occurs rather early. If the source and receiver are in the same room, Π and r in Eq. (16) have the conventional interpretations, but if they are in separate rooms both the source, if it is visible, and the coupling aperture behave as sources of the reverberant field in the room not containing the source. To address this requires greater revision of Eq. (8) than that given in Eq. (16).

D. Limitations of and corrections to the improved model

1. Strength of coupling

SA models of coupled rooms are most accurate when applied to systems that are not strongly coupled.[13–18] Strongly coupled systems are defined by equipartition of energy whereas weakly coupled systems are defined by subsystems that behave as though isolated.[28] The intermediate case is that of loosely coupled rooms. In such systems, the steady-state levels and decay processes can only be described by a theory that accounts for the exchange of energy between the spaces. Based on these definitions, Smith[28] has given the criterion for strong coupling in a two-room system as $\kappa>1$, where

$$\kappa=\frac{S_{ij}}{A_{i0}}+\frac{S_{ji}}{A_{j0}}, \tag{17}$$

(where $S_{ij}=S_{ji}$ for the two-room case). Cremer and Müller[14] presented a similar criterion for two-room systems described by the coupling factor

$$k_j=\frac{S_{ji}}{A_{j0}+S_{ji}}. \tag{18}$$

For a source in the ith room, strong coupling is defined by $k_j\sim 1$ and weak coupling is defined by $k_j\sim 0$. Note that, by Smith's definition, two rooms are strongly coupled if either k_i or $k_j>0.5$. This is a stricter formulation of Kuttruff's guideline that the SA model of coupled rooms is applicable to those cases where the energy lost via coupling is not substantially larger than the energy lost via absorption.[17]

Lyle[15] has proposed an empirically derived upper limit for the accurate application of the SA model based on the idea of coupling strength

$$\max S_{ij}=\min M(0.4-\overline{\alpha_i})S_i \quad \text{for } \forall i,j, \tag{19}$$

where $M\leqslant 1$ is the "mixing constant." In ideally diffuse rooms $M=1$ and, for apertures above the limit, the system can be treated as a single room. In rooms that are not ideally diffuse $M<1$ and no model can be certain to work for the strong-coupling condition. In such cases, equipartition of energy between the now unified subrooms may not occur even though the system is, geometrically, a single space.[15]

Each of these criteria is fallible. In comparisons with GA, Eq. (17), often predicts that the model should fail before it does. In contrast, Eqs. (18) and (19) often fail to predict that single-volume rooms should be treated as such.

2. Failure of statistical assumptions

Progressive discrepancy between predictions of GA and SA as rooms become more strongly coupled is partly due to violations of the additional assumptions made by the SA model of coupled rooms, as given in Sec. II B.

Coupling apertures on the boundaries of subrooms violate the assumption that decay properties of individual rooms are unaltered by coupling. Geometrical averaging of absorption coefficients can be understood to originate in the multinomial distribution describing the number of reflections that occur from each surface of an enclosure in the case of independent reflections.[17] Though this assumption is never fully correct,[2] especially for specular reflection,[6] it is further flawed if any portion of the surface, such as a coupling aperture, is perfectly absorptive. If a phonon travels out of an aperture, the next reflection will not occur in the original room and the two successive reflections are dependent. This leads to flaws in the averaging of the absorption coefficients because an aperture diminishes the probability that all room surfaces will be uniformly sampled, as Eyring first observed.[19]

Large apertures, because they act initially as perfect absorbers, cause anisotropy in the sound field due to the establishment of a net flow of energy (i.e., there are fewer phonons moving away from the aperture than toward it[2]). If the aperture area is not too large, SA models can still describe the behavior.[1,6] However, if the area is too large, SA models will fail as the preferential selection of trajectories by the aperture slows the mixing process.[6]

Locations and sizes of the apertures also affect free-path distribution. Unless conditions are such that the Sabine model is valid, the decay associated with the room will vary as a function of the location of apertures. Even if free-path distribution as modified by the apertures is known for each of the subrooms, distributions will differ when the rooms are coupled due to interaction of the subrooms. Certain free paths that are not available in either of the subrooms are made possible in the coupled system. Therefore, the eigenvalue decay rates will not be exactly those derived from the uncoupled decay rates because coupling the two rooms will shift the natural decay rates of the rooms by changing the shapes of the free-path distributions.

3. Nondiffuse transfer of energy

The first assumption of the SA model, that there is an abrupt transition at the coupling aperture between unique diffuse sound fields, is also not accurate. Sound radiates from the coupling aperture with energy density that is distinct from the energy density of the reverberant field of the room into which it radiates. Therefore, it behaves, initially, as a direct-sound component. Only after it has undergone reflection is it part of the reverberant field. This phenomenon has been observed for rooms coupled by partially transondent partitions[13] and for rooms coupled by apertures.[19] Assuming a diffuse field in the source room at a large distance r from the aperture the finite dimensions of the aperture can be neglected and the aperture is approximated by a Lambert

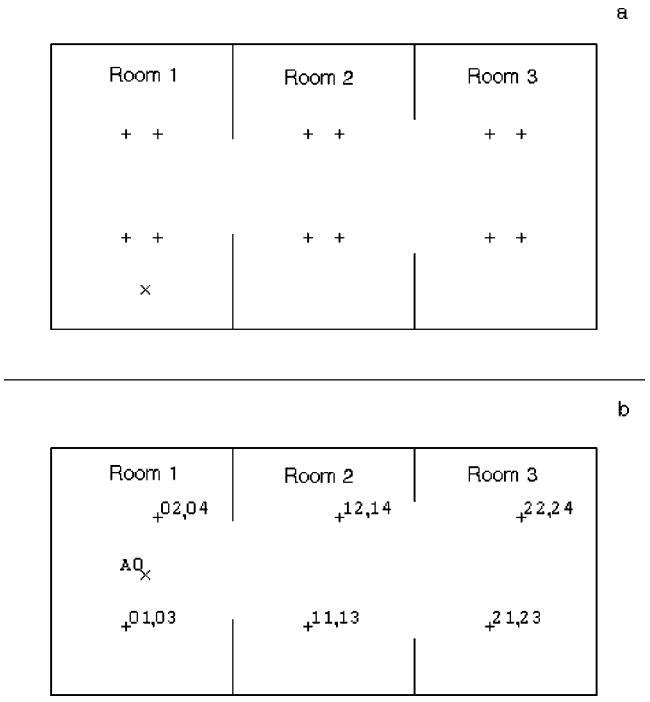

FIG. 1. Three-room coupled system first studied by Kuttruff. Transverse section (a) and plan (b) views are shown. Volumes V and areas S are the same for each subroom: $V=6270$ m^3 and $S=2066$ m^2 15 m$\times$19 m $\times$22 m); areas include coupling areas. Crosses (+) indicate receiver positions: 1–4 in Room 1, 11–14 in Room 2, and 21–24 in Room 3. The single source position in Room 1, A0, is indicated by an X.

source[17] of power $B_i S_{ij}$. If the locally planar assumption is met, the energy density in room j due to the direct contributions from an aperture, ε_j, is

$$\varepsilon_j(\mathbf{r},t)=\frac{\cos(\theta)S_{ij}\varepsilon_i(t)}{4\pi r^2} \tag{20}$$

for an aperture coupling the jth room to the ith room, where $\mathbf{r}$ is the position vector of the receiver in the jth room (with magnitude r), θ is the angle from the normal to the wall containing the aperture, and $\varepsilon_i(t)$ is the energy density of the ith room. This implies that, in regions near coupling apertures, direct radiation from adjacent rooms can dominate the sound fields of rooms with lower energy density than those adjacent rooms.

Because energy transmitted through coupling apertures is first radiated as a quasidirect component, reverberant energy can be transferred between rooms that are not adjacent. This is illustrated by considering the system of three coupled rooms shown in Fig. 1 that was first studied by Kuttruff.[17] Traditional analysis assumes $S_{13}=S_{31}=0$. However, a certain portion of the sound radiated from S_{12} will pass through S_{23} before undergoing a reflection in room 2. Likewise, a portion of the sound radiated from S_{32} passes directly through S_{21}. If the radiation from the aperture has an angular distribution given by Eq. (20), the fraction of the sound power radiated by S_{12} that passes directly through S_{23} (or vice versa), is given by the radiation shape factor between the two apertures

$$F_{13}=F_{31}=\frac{1}{\pi S_{12}}\int_{S_{12}}\int_{S_{23}}\frac{\cos\phi_{12}\cos\phi_{23}}{r^2}dS_{12}dS_{23}, \tag{21}$$

where r the magnitude of the vector between points on the aperture surfaces and ϕ_{ij} are the angles between the vector connecting the points and the normals of S_{ij}. Having determined the fraction of energy transmitted directly between the apertures, the corrected coupling areas are given by

$$\begin{aligned} S'_{12}&=(1-F_{13})S_{12},\\ S'_{32}&=(1-F_{13})S_{32},\\ S'_{13}&=F_{13}S_{12},\\ S'_{31}&=F_{13}S_{32}. \end{aligned} \tag{22}$$

This approach can be extended to more complex geometries. For example, a room with multiple apertures, which is not convex in the region containing the apertures, may have F_{ii} that is nonzero. Given simple configurations and aperture shapes, the radiation shape factors can be calculated directly (see the appendix A of Ref. 25). In more complex geometries, they must be determined computationally. In such cases it is possible to form rough estimates of the factors from ratios of surface areas of the apertures to the total surface areas of the rooms.

4. Spatial variation

Equation (16) suggests a correction to the basic theory as the level of the reverberant energy density at the coupling aperture may differ from the value used in Eq. (11). Thus B in the prior derivation should be modified if B is the irradiation strength in a room containing a source. Even in rooms that do not contain a source, the aperture itself acts as a source so that spatial variation may result. The spatial variation in the level of the reverberant energy suggests that spatial variation in decay shape may occur under certain conditions because the multiplier terms in Eq. (14) will be functions of position.

III. GEOMETRICAL-ACOUSTICS MODEL

The exact GA solution for the energy decay can be obtained through the solution of an integral equation.[4,17,29] In practice, GA solutions are obtained computationally using ray tracing or its variants, which can be viewed as Monte Carlo approximations to the exact solution.[30]

In this study, the geometrical-acoustics software CATT-Acoustic V. 8.0 is used.[31,32] Nonspecular reflection is modeled as Lambert diffuse reflection,[17] for which scattering coefficients s are defined as the fraction of energy that is not specularly reflected. While angular dependence of absorption coefficients is not accounted for, it can be safely neglected for large, reverberant enclosures having sufficiently large scattering coefficients.[33,34] The original algorithm assumes a constant, quadratic rate of growth of the reflection density, which is not true in certain coupled rooms.[35] To address this, a new version of the algorithm[35] (introduced in commercial versions 8.0b and above) is used.

IV. COMPARISON OF STATISTICAL AND GEOMETRICAL ACOUSTICS

In order to characterize the relationship between SA models and GA models of coupled-room systems, two- and three-room coupled systems are studied. In the two-room geometry, the volumes of the subrooms are based on averages of performance spaces which employ either a coupled stage house or an auxiliary coupled chamber. The predictions of decay curves and steady-state energy densities given by SA and GA are compared for each of the rooms under a series of different conditions of the room surfaces. The purpose of these simulations is to determine how the additional assumptions implicit in SA models of coupled rooms affect the relationship of their predictions with those of GA. By comparing predictions of energy decay and steady-state energy density, conditions for which the GA model is approximated by SA models are assessed in terms of degree of coupling and absorption and scattering coefficients of the surfaces of the subrooms. The three-room geometry is taken from previous work conducted by Kuttruff[17] and serves to evaluate elements of the new model that improve the accuracy of predictions in systems having more than two rooms. In both two- and three-room geometries the subrooms are modeled as rectangular parallelepipeds, which, though not ergodic given specular reflection,[3,29] are both ergodic and mixing for $s>0$.

A. Methodology

The GA computer model is used to generate energy echograms for each source-receiver combination. Time-ensemble-average decay curves $\langle s(t)\rangle$ for fixed source-receiver pairs are derived by Schroeder integration of energy echograms and steady-state energy-density values are taken from maxima of these integrated echograms. Steady-state energy-density values are plotted as a function of the distance of the receiver from the source, a so-called sound-propagation curve, and compared with predictions of the SA model. For comparison with SA predictions of decay rate, spatial averaging is used to more accurately describe global characteristics of the sound field within each subroom. Space-ensemble-average decay curves $\{\langle s(t)\rangle\}$ are calculated by synchronous averaging of $\langle s(t)\rangle$ over receiver and/or source positions.[36] The number of source and receiver positions is chosen in accordance with the recommendations given in Ref. 37.

The mean-free path $\langle\overline{\ell}\rangle$, averaged both over the time history of each cone/ray and over the ensemble average of all the cones/rays, is calculated from the trajectories of all the cones/rays emitted from a given source position according to

$$\langle\overline{\ell}\rangle=\frac{1}{M}\sum_i \langle\ell\rangle_i=\frac{1}{MN}\sum_{ij}\ell_{ij}, \tag{23}$$

where ℓ_{ij} is the length of the jth path taken by the ith cone/ray, M is the total number of cones/rays, and N is the total number of paths traced per cone/ray.

Fitting sums of decaying exponentials to decay curves by a least-square method is ill conditioned. Therefore, specifying the difference between two models in terms of rms error is not generally meaningful. Instead, decay curves are compared visually. In some cases, the decay parameters predicted by SA are compared with those extracted from the decay curve predicted by GA using Bayesian parameter estimation.[38]

B. Uncertainty analysis

In comparing SA predictions with GA predictions, there are two sources of uncertainty (1) u_a, uncertainty of the model outputs due fluctuations in the algorithm, which applies to the computational GA model only, and (2) u_i, uncertainty of the model outputs due to uncertainty in the inputs, which applies both to GA and SA models. Only u_a directly concerns the comparisons made here, because the input parameters for the models are known exactly. However, in practice both models will be evaluated on their ability to predict reality. In that case, the relative sensitivity of the GA and SA models to uncertainty in the input parameters determines whether one model is more accurate than the other.

1. Algorithmic uncertainty

As discussed in Sec. III, CATT-Acoustic yields Monte Carlo approximations to the exact GA solution which display stochastic run-to-run fluctuations. For simple algorithms, analytic estimates of u_a exist.[38] For CATT-Acoustic, no uncertainty estimate has been developed; therefore u_a in each case is estimated from the standard deviation of ten predictions. This uncertainty is larger at later times and smaller for larger numbers of cones/rays. Many cone/rays were used for the simulations such that, for $\{\langle s(t)\rangle\}$, $u_a\ll 1$ dB. Because of this, u_a is not plotted along with results and can be assumed negligible.

2. Input uncertainty

Real input parameters, including room geometry and surface parameters, are known to finite precision. Comparative merit of the modeling approaches can be practically assessed only in terms of u_i, uncertainties of predictions due to uncertainties of input parameters. Consideration here is limited to input parameters whose uncertainty is of most significance: absorption and scattering coefficients, which may have uncertainties of 10% or more.

For small numbers of subrooms, it is tractable to solve the SA model algebraically and therefore possible to develop analytical expressions for u_i.[39] In general, Eqs. (11) and (15) are solved numerically. Uncertainty in the final predictions is estimated (up to first-order terms in a Taylor-series expansion) by computing influence coefficients for each input parameter at the limits of its region of confidence.[39] While this is in error if the predictions are a nonlinear function of the input parameters,[40] this linear approximation, which also neglects interactions between the input parameters, is reasonable for small uncertainties.

A similar procedure is applied to estimate u_i in the GA model. Though the additional input parameter s makes the assumption of noninteraction less plausible, the alternative—Monte Carlo estimation of the distribution of the output data—is too time consuming. Variations in s for $s>0.5$ typi-

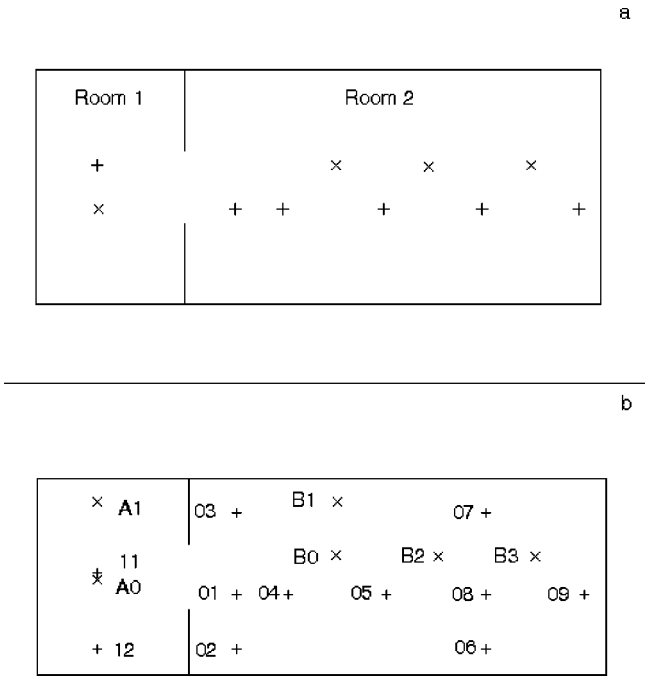

FIG. 2. Two-room coupled system. Transverse section (a) and plan (b) views are shown. The volumes V and areas S of the subrooms are $V_1 = 6270\ \mathrm{m}^3$, $S_1 = 2066\ \mathrm{m}^2$ (15 m×19 m×22 m) and $V_2 = 17\,556\ \mathrm{m}^3$, $S_2 = 4280\ \mathrm{m}^2$ (42 m×19 m×22 m) and; areas include coupling areas. Crosses (+) indicate receiver positions: 1–9 in Room 2, 11–14 in Room 1. Sources are indicated by X's: A0-A1 in Room 1 and B0-B3 in Room 2.

cally have little influence on decay curves.[7,21] Therefore, in many cases (and most of the cases of interest here) keeping only the linear term of the Taylor series is a reasonable approximation.

C. Two-room system

A simplified representation of a concert hall with an auxiliary coupled room is constructed by positioning the auxiliary volume, Room 1, along the short side of the audience chamber, Room 2, as shown in Fig. 2. Source positions in Room 1, A0-A1, and Room 2, B0-B3, are considered. A total of 11 receiver positions are simulated for each of the seven source positions. As shown in Fig. 2, nine of the receivers, labeled 1–9, are distributed within Room 2 and the remaining two receivers, labeled 11, 12, are located in Room 1. The rooms are coupled by a single aperture centered in the wall separating them. Four aperture sizes, 25, 50, 100, and 200 m^2 are used. The aspect ratio of each is one. For each geometrical condition three different absorption conditions are modeled: (1) uniform absorption ($\alpha = 0.10$) for all wall surfaces, (2) uniform α for wall surfaces within each subroom ($\alpha_1 = 0.10$, $\alpha_2 = 0.20$), such that the absorption power in Room 2 is equivalent to that presented by an audience, and (3) a similar condition in which the increase in the absorption of Room 2 is affected by increasing the absorption coefficient of the floor surface to 0.80 in order to simulate the nonuniform absorption presented by an audience and all other surfaces are assigned $\alpha = 0.10$. For each absorption condition there are three scattering conditions for which Lambert scattering coefficients $s = 0.10$, 0.60 and 0.99 are applied to all surfaces uniformly.

Coupling strengths are calculated according to the criteria described in Sec. II D 1. Equation (17) predicts that the coupling is strong in all cases for which $S_{12} \geqslant 100\ \mathrm{m}^2$. By contrast, Eqs. (18) and (19) predict that the system is never strongly coupled, even when configured as a single room.

For Condition 1, much of the relationship between SA and GA predictions is known from previous studies of single-volume rooms. Thus, comparison is made only between the improved SA model using the Kuttruff decay model ($\eta = \alpha''/\overline{\alpha}$) within the subrooms and GA. Predictions of Knudsen's conjecture using Eyring and Kuttruff models are then similarly compared with GA predictions. For Conditions 2 and 3, the improved-SA-model decay-curve predictions using Sabine ($\eta = 1$), Eyring ($\eta = \alpha'/\overline{\alpha}$), and Kuttruff ($\eta = \alpha''/\overline{\alpha}$) decay models within the subrooms are compared with GA predictions. Condition 3 also allows for the Kuttruff–Embleton decay model ($\eta = \alpha'''/\overline{\alpha}$) to be used in Room 2. For each condition, the predictions of Eq. (16) are compared with sound-propagation curves calculated by GA. In the case of Conditions 2 and 3 the influence of this on the spatial variation of decay-curve shape is shown.

1. Condition 1: Uniform absorption

Given uniform absorption, Room 1 is less reverberant than Room 2 and, thus, single-slope decay curves result in Room 2 if the source is located in that room, while in Room 1 the initial slope of the decay is zero and over time approaches the slope of the decay curve in Room 2, as shown in Fig. 3. Also shown in Fig. 3, as the size of the coupling aperture increases, initial levels of decay curves approach each other and the initial transition period of the decay in Room 1 becomes shorter. It is this condition of sources in Room 2 that is analyzed below.

As expected, the improved model using the Kuttruff decay model within the subrooms accurately predicts decay curves, as illustrated in Fig. 3 for $S_{12} = 25$ and 200 m^2. In comparison (though, for clarity, not shown in Fig. 3), the Sabine decay model slightly underpredicts the decay rates and the Eyring decay model slightly overpredicts the decay rates. For $S_{12} \leqslant 100\ \mathrm{m}^2$ there is little variation in the accuracy of the predictions of the SA model with aperture size. As shown in Fig. 3, the error increases markedly for $S_{12} = 200\ \mathrm{m}^2$. The reasons for this have been discussed in Sec. II D 2. As shown in Fig. 4, $\langle \overline{\ell} \rangle$ of the uncoupled subrooms decrease from $4V/S$ (Room 1:12.1 m, Room 2:16.4 m) as the size of the aperture is increased due to an increase in the relative frequency of short paths. Increasing the size of the aperture also allows increased access to long-length paths associated with the coupled system as a whole. The longest free path available in Room 2 is 51.08 m. Figure 4 shows that as the aperture size increases the relative frequency of path lengths in the coupled system greater than 51.08 m also increases. The net effect of these phenomena is an increase in γ^2 of the subrooms. Because increased γ^2 decreases the decay rate of a room, overprediction of the decay rates in the subrooms is made more severe as aperture size increases. Increase in γ^2 depends on the geometry of room. However, there is not a known relationship between γ^2 and aperture size for a fixed geometry or between geometry and rate in-

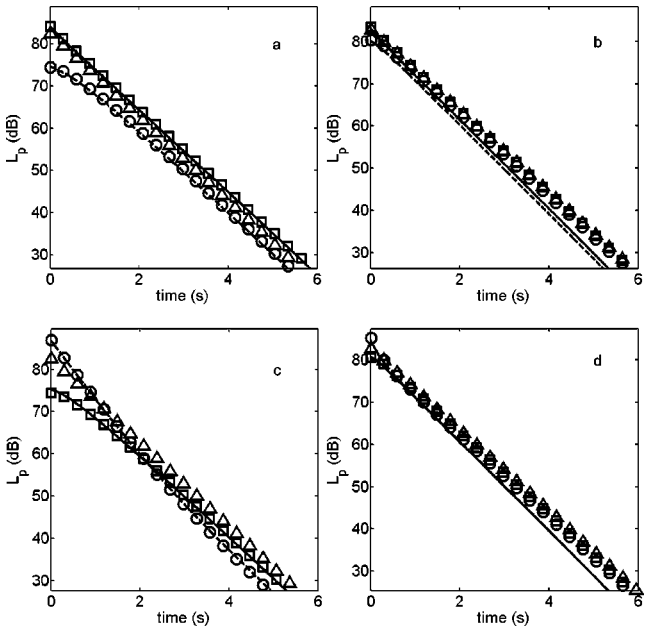

FIG. 3. For the two-room coupled system (Fig. 2) in Condition 1, spatial averages of GA-model predictions ($s=0.99$) for receivers in Room 1 (dashed line) and Room 2 (solid line) are compared with improved-SA-model predictions using Kuttruff's decay model within the subrooms [Eq. (11), $\eta=\alpha''/\overline{\alpha}$] for Room 1 (circles), Room 2 (squares), and the Kuttruff form of Knudsen's conjecture [Eq. (9) using α''] (triangles). Ensemble averages of all source positions in Room 2 with $S_{12}=25\ \mathrm{m}^2$ (a) and $200\ \mathrm{m}^2$ (b) and in Room 1 with $S_{12}=25\ \mathrm{m}^2$ (c) and $200\ \mathrm{m}^2$ (d) are shown.

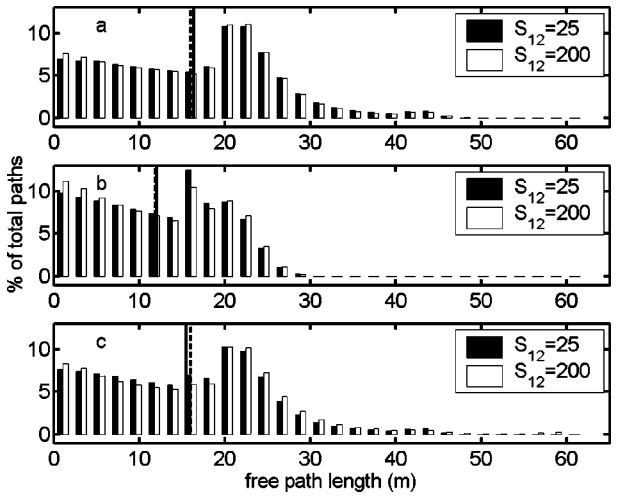

FIG. 4. For the two-room coupled system (Fig. 2), free-path distributions of cones/rays emitted (a) from source B2 in isolated Room 2 with $S_{12}=25\ \mathrm{m}^2$ (black bars) and $200\ \mathrm{m}^2$ (white bars) simulated by absorbing patches, (b) from source A0 in isolated Room 1 with $S_{12}=25\ \mathrm{m}^2$ (black bars) and $200\ \mathrm{m}^2$ (white bars) simulated by absorbing patches, and (c) from source B2 in the coupled system with $S_{12}=25\ \mathrm{m}^2$ (black bars) and $200\ \mathrm{m}^2$ (white bars) are shown. Mean-free paths are indicated by vertical lines for $S_{12}=25\ \mathrm{m}^2$ (solid lines) and $200\ \mathrm{m}^2$ (dashed lines).

crease in γ^2 with aperture size. Instead increase can be accounted for heuristically by multiplying γ^2 by a correction factor. Factors $\sim$1–2 have been found to work well for this particular coupled system. These observations and corrections hold generally for this coupled system because absorption configurations with $\alpha<1$ do not alter the free-path distribution.

Bayesian analysis gives additional insight into phenomena observed. For $S_{12}\leqslant 100\ \mathrm{m}^2$ the two rates extracted from the decay curves computed by the GA computer model approximately agree with the decay rates predicted by the SA model. The differences between the rates predicted by the models increase as the aperture size increases. In the case of $S_{12}=200\ \mathrm{m}^2$, with the source in Room 1, Bayesian analysis supports three decay rates. The first rate is associated with Room 1 and is similar to the SA prediction. The other two rates, which correspond to reverberation times of 6.10 and 6.40 s, may correspond, respectively, to the decay rate associated with Room 2 or the decay rate associated with the entire coupled system. The rate associated with Room 2 has a platykurtic posterior probability distribution and is only weakly supported by the data. As the decay curves shown in Fig. 3 suggest, the system is at the point of transition between one- and two-room behaviors.

GA predictions are also compared with Knudsen's conjecture [Eq. (9)]. As determined by GA, $\langle\overline{\ell}\rangle$ of the coupled system differs little from $4V/S$ ($S_{12}=25\ \mathrm{m}^2$: $\langle\overline{\ell}\rangle=15.5$, $4V/S=15.1$; $S_{12}=200\ \mathrm{m}^2$: $\langle\overline{\ell}\rangle=16.0$, $4V/S=16.0$). Differences increase for small coupling apertures due, most likely, to increase in mixing time of the geometry such that $\langle\overline{\ell}\rangle=4V/S$ is not satisfied within the truncation time of the computation. Using the Eyring decay model, Knudsen's approach overpredicts the decay rate. But, by accounting for γ^2, the Kuttruff form of Knudsen's conjecture becomes rather accurate, as shown in Fig. 3. The remaining error is primarily the incorrect prediction of equipartition of energy. Therefore, Knudsen's conjecture becomes more accurate as S_{12} increases.

For sources and receivers both in Room 2, the steady-state energy density is well predicted by the modified form of Barron and Lee's revised theory using $\eta=\alpha''/\overline{\alpha}$ (errors <1 dB), as shown in Fig. 5 for Source B3. As expected, errors increase for higher s due to backscattering. Equation (16) suggests that the level of the reverberant field should decrease linearly with distance at a single rate determined by the dominant decay rate in Room 2. But, due to backscattering, there are two distinct rates; one associated with the receivers near the source (1–5) and a second associated with the receivers far from the source (6–9).

2. Condition 2: Uniform absorption within each subroom

When loosely coupled, the system displays for these absorption conditions the strongly nonlinear decay curves typically associated with coupled rooms.

The GA model predicts that the decay rate of the late portions of the decay curves decreases with time for $s=0.10$. This is especially notable for $S_{12}\geqslant 100\ \mathrm{m}^2$. In cases for which the late decay is not dominated by long-lived paths ($s=0.60,0.99$), using the Kuttruff decay model ($\eta=\alpha''/\overline{\alpha}$) in the improved SA model most accurately predicts the decay curves, as shown in Fig. 6, while Sabine ($\eta=1$) and Eyring ($\eta=\alpha'/\overline{\alpha}$) decay models used in the improved SA model underpredict or overpredict the decay rates, respectively. The Kuttruff decay model tends toward overprediction of these decay rates, which is greater for larger S_{12} and can be attrib-

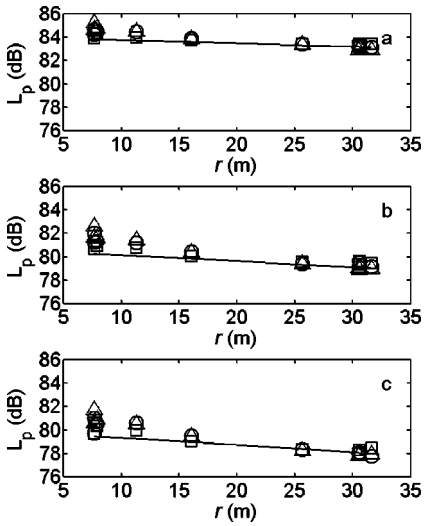

FIG. 5. Sound propagation curves (with direct sound subtracted) in Room 2 for Source B3 and $S_{12}=25\ \mathrm{m}^2$ in Conditions 1 (a), 2 (b), and 3 (c) computed by the GA model for $s=0.10$ (squares), 0.60 (circles), and 0.99 (triangles) are compared with the predictions of Eq. (16) (solid line).

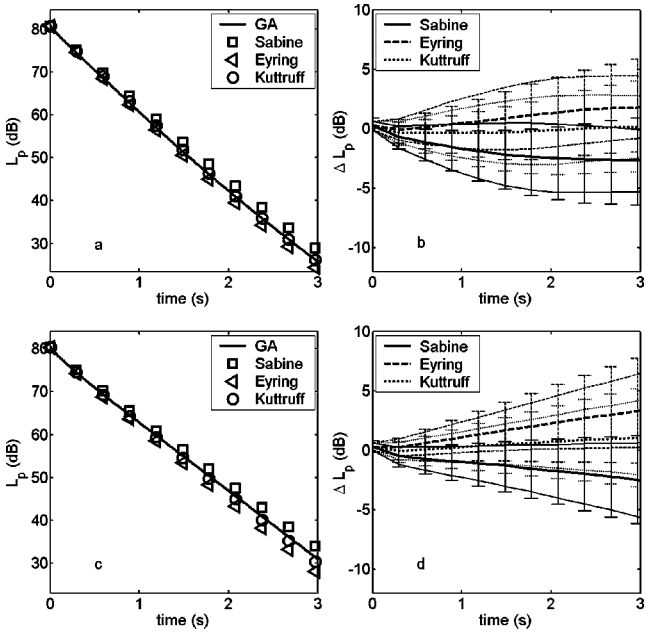

FIG. 6. For the two-room coupled system (Fig. 2) in Condition 2, ensemble averages of GA-model predictions ($s=0.99$) for all sources and receivers in Room 2 (solid line) are compared with improved-SA-model predictions using Sabine [Eq. (11), $\eta=1$] (squares), Eyring [Eq. (11), $\eta=\alpha'/\overline{\alpha}$] (circles) decay models within the subrooms for $S_{12}=25\ \mathrm{m}^2$ (a) and 200 m^2 (c). Differences between GA and SA predictions ($10\log_{10}\mathrm{GA}-10\log_{10}\mathrm{SA}$) [using Sabine (solid line), Eyring (dashed line), and Kuttruff (dotted line) decay models] are plotted for $S_{12}=25\ \mathrm{m}^2$ (b) and 200 m^2 (d). The regions of confidence defined by u_i are plotted as error bars for SA predictions and as fainter lines lying on either side of the primary lines for GA predictions. Confidence limit predictions assume α and s are known to $\pm 10\%$ at the same level of confidence.

uted to increased variance of the free-path distribution, as observed in Sec. IV C 1. Multiplying γ^2 by a correction factor can address this error. As shown in Fig. 6, the GA model is typically less sensitive to input uncertainty. For uncertainty in α and s of $\pm 10\%$, the confidence limits of the predictions are such that all of the models can be considered equally accurate.

Section II D 4 suggests that spatial variation in the shape of the decay curve may occur as a result of spatial variation in the energy density associated with each eigenfunction. Such variation should be most significant for Source B3, for which the difference in the distance between the source and a given receiver and the aperture and a given receiver is greatest. Instead, the GA model predicts little spatial variation. The level and rate of the late decay vary somewhat with position (as shown in Fig. 5), but the decay curve maintains the same basic shape, as shown in Fig. 7. As before, the level of the reverberant field decreases with distance from the source, as shown in Fig. 5. Because δ_1 is larger, the rate of decrease is greater, as Eq. (16) predicts. However, the increase in level near the source for large s, which is not predicted by the model, is also larger and steeper in slope. This variation is not due to the nonlinearity of the decay curve predicted by the SA model, because over the time range relevant here ($\leqslant$150 ms) the decay curve is essentially single sloped. Instead, it can be attributed to the additional absorption in Room 2.[25]

3. Condition 3: Simulated audience absorption

Because of nonuniform distribution of absorption in Room 2, for $s<0.40$ reasonable accuracy of SA models cannot be assured.[21] In Room 2 there is a balance between long-lived paths and anisotropy of the sound field.[35] For small s, long-lived paths and two-dimensional reverberation dominate, resulting in a nonlinear decay curve of the room when uncoupled. For higher scattering coefficients, the enclosure is more mixing, so the effects of anisotropy dominate.

Because of this, the improved SA model using Sabine model of decay in the subrooms ($\eta=1$) underpredicts the decay rate in Room 2 for all aperture conditions. The Embleton model suggests that the Eyring model should also underpredict the decay rate in Room 2. The combination of an increase in the decay constant due to anisotropy and a decrease in the decay constant due to variance in the free-path distribution tend to negate one another in this particular case, producing a decay curve in the primary room that agrees with the prediction of the improved SA model using the Eyring model of decay in the subrooms ($\eta=\alpha'/\overline{\alpha}$). This is confirmed by employing the Kuttruff–Embleton decay model ($\eta=\alpha''''/\overline{\alpha}$), which predicts the decay rate well in Room 2. Figure 8 illustrates the comparisons made above. In Room 1 the behavior is the same as in the previous cases and the Kuttruff model ($\eta=\alpha''/\overline{\alpha}$) gives the most accurate prediction of the decay rate. The GA model is seen in Fig. 8 to be less sensitive to input uncertainty, as observed for Condition 2. However, overall errors are greater than Condition 2 and the different decay models cannot be considered equally accurate for input uncertainties of $\pm 10\%$.

As in Condition 2, Eq. (16) predicts the propagation curves well, with larger errors for higher values of s, as shown in Fig. 5. While the energy propagation curve is similar to the previous case, the spatial variation of the decay curve shape is greater. As shown in Fig. 7, Receivers 1–5 start at lower levels than Receivers 6–9, because they are further from the source, but end at higher levels, because

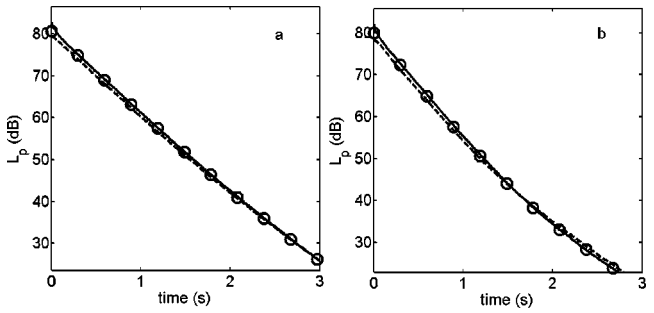

FIG. 7. For the two-room coupled system (Fig. 2) with $S_{12}=25\ \mathrm{m}^2$ and Source B3, spatial variation in decay shape is shown between ensemble-averaged decay curves of receivers 1–5 (dashed lines), far from the source, and 6–9 (solid lines), near the source, given absorption Condition 2, with $s=0.99$ (a), and absorption Condition 3, with $s=0.99$ (b). The predictions of the improved SA model [Eq. (11) with $\eta=\alpha''/\overline{\alpha}$, for Condition 2, and with $\eta=\alpha'''/\overline{\alpha}$ for Condition 3] are shown for reference (circles).

they are nearer to the coupling aperture. In an actual room the effect may be more marked due to grazing-incidence attenuation, which is not accounted for by the GA model.

D. Three-room system

SA calculations of the decay curves in a system of three coupled rooms have been discussed previously by Kuttruff.[17] Because the three-room model studied by Kuttruff was computed only by SA, all of the room parameters were not given explicitly. Taking the three rooms of equal volume to be geometrically identical, Kuttruff's specifications are $\alpha_2=\alpha_1/10$, $\alpha_3=\alpha_1/2$, $S_{12}=S\alpha_1/20$, and $S_{23}=S\alpha_1/10$, where S is the area of each room, inclusive of the aperture area. As shown in Fig. 1, the rooms are chosen to be of the size and shape of Room 1 of the previous geometry and are coupled through their largest wall with a square aperture centered in each interior dividing wall. The absorption coefficients are determined by specifying that $\alpha_1=0.50$, which results in a reverberation time of approximately one second in Room 1. Kuttruff's conceptual model of three rooms did not specify the distribution of absorption within the subrooms; thus, the absorption is uniformly distributed.

Four receivers are modeled in each room, as shown in Fig. 1. The decay curves computed for the four receivers in each room are ensemble averaged to give $\{\langle s(t)\rangle\}$ for that room. A single source position, located in Room 1, is modeled. The solid angle subtended by S_{12} as viewed from the source is computed in order to evaluate the initial power distribution.

The configuration shape factor of the two apertures S_{12} and S_{23} is determined according to Eq. (21). An adaptive Gaussian-quadrature routine is used to evaluate the four-dimensional integral. Note that Receivers 11 and 12 are in the direct path of the transmission between Room 1 and Room 3. Therefore, they are affected by the transmitted energy as it passes them. While this may appear problematic, removing the receivers from the ensemble average in Room 2 alters the decay-curve level only a small amount ($\sim$0.2 dB).

Comparing the predictions of the improved SA model [Eq. (11), $\eta=\alpha''/\overline{\alpha}$, with additional corrections discussed above] and Kuttruff's original model [Eq. (11), $\eta=1$, without additional corrections] with those of GA indicate that the improved model yields significantly more accurate predictions, as shown in Fig. 9. Conservative uncertainty estimates of $\pm 10\%$ for each α yield only slight overlap between the two SA models suggesting that their prediction will be significantly different in actual circumstances. The sensitivity of the GA model to input uncertainty is somewhat lower than the SA models, for this geometry. As a result, the predictions of the improved SA model and GA are identical given the 10% uncertainty in all the input parameters (α and s).

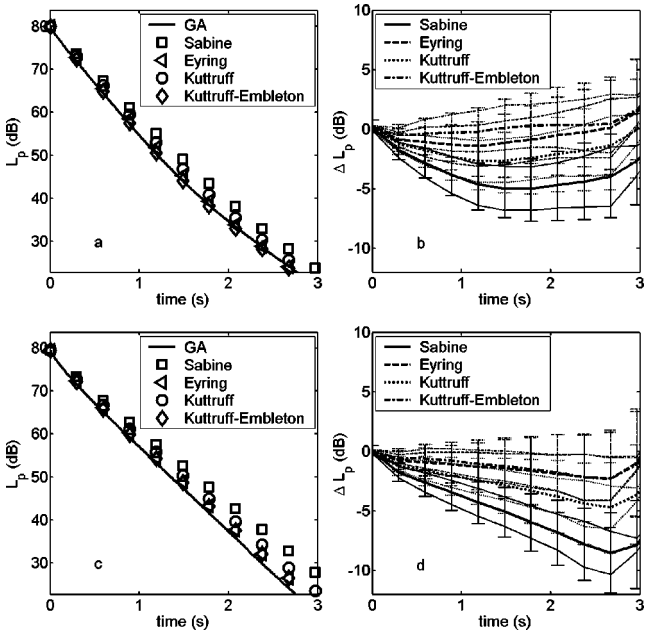

FIG. 8. For the two-room coupled system (Fig. 2) in Condition 3, ensemble averages of GA-model predictions ($s=0.99$) for all sources and receivers in Room 2 (solid line) are compared with improved-SA-model predictions using Sabine [Eq. (11), $\eta=1$] (squares), Eyring [Eq. (11), $\eta=\alpha'/\overline{\alpha}$] (triangles), and Kuttruff [Eq. (11), $\eta=\alpha''/\overline{\alpha}$] (circles) decay models within the subrooms for $S_{12}=25\ \mathrm{m}^2$ (a) and 200 m^2 (c). Differences between GA and SA predictions ($10\log_{10}\mathrm{GA}-10\log_{10}\mathrm{SA}$) [using Sabine (solid line), Eyring (dashed line), and Kuttruff (dotted line) decay models] are plotted for $S_{12}=25\ \mathrm{m}^2$ (b) and 200 m^2 (d). The regions of confidence defined by u_i are plotted as error bars for SA predictions and as fainter lines lying on either side of the primary lines for GA predictions. Confidence limit predictions assume a and s are known to $\pm 10\%$ at the same level of confidence.

The improvement over the prior model can be attributed to multiple factors. First, the improved model incorporates more accurate decay models. In this system the decay curves in all of the rooms are dominated by the rates associated with Rooms 1 and 2. Bayesian analysis of the decay curves computed by the GA model does not support the extraction of a decay rate associated with Room 3. Nevertheless, comparing the predictions of the statistical models with the extracted decay rates for various scattering coefficients indicates that using the Kuttruff decay model ($\eta=\alpha''/\overline{\alpha}$) within the improved SA model is most consistently accurate. Second, the improved model incorporates the Vorländer model of steady-state energy density [Eq. (7)], which is less prone to overestimation than the Sabine model used in prior work. Finally, the improved model accounts for the nondiffuse transfer of energy between Rooms 1 and 3. The impact of this correction is most notable in an improvement in the accuracy of the decay curve predicted in Room 3. Without this correction,

the improved model cannot accurately predict the early part of this decay curve.

In contrast with these findings, the solid-angle correction for the initial power distribution does not give a consistent improvement. While it does improve the fit of the SA model to the GA prediction in Room 1 (by decreasing the level of the decay associated with Room 1 and increasing the level of the decay associated with Room 2), it results in overprediction of the levels in Rooms 2 and 3.

A significant factor in this system of rooms is that the receivers are near the apertures. As such, the considerations described in Sec. II D 3 can be made for each receiver.

Finally, it should be noted that this geometry violates Eq. (19), because $\alpha_1 > 0.40$. However, repeating the previous work with $\alpha_1 = 0.30$ does not notably alter the conclusions drawn.

V. CONCLUDING REMARKS

A. Observations

The accuracy of SA models of coupled rooms is greatly influenced by the accuracy of the SA model used to estimate decay rates in the subrooms of the coupled system. Criteria required for SA models to be approximately correct in single-volume rooms must be met in each of the subrooms if SA models of coupled rooms are to be used. Surface scattering is neither necessary nor sufficient to ensure the agreement of SA predictions with those of GA. Increasing the amount of surface scattering in a room that does not otherwise satisfy the conditions of diffuse-field models tends to improve agreement with the predicted decay rate but, once a linear decay curve has been achieved, increases in surface scattering will not necessarily improve the agreement with a given statistical model.

Stronger coupling increases the disagreement between SA and GA. Previously introduced guidelines for the conditions under which SA models can be used conflict with one another and with comparisons to GA. The possible causes for the failure of SA models are sufficiently interconnected and diverse that a single criterion cannot predict the conditions for failure. Particularly, previous guidelines have been based purely on SA and therefore neglect causes of failure that are rooted in GA, as discussed in Sec. II D.

In systems of coupled rooms, the decrease in level of the reverberant field with distance can be predicted by a modified form of Barron and Lee's revised model. For such systems, this variation in the level of the reverberant field can result in spatial dependence in the shape of the decay curve. This effect is most significant when the coupling aperture and the source are in disparate locations. In contrast, decay curves vary spatially in level but not in shape if the source is located near the coupling aperture.

Unlike prior work, the improved SA model introduced here accounts for the nondiffuse transfer of energy due to (1) radiation of the source into adjacent subrooms and (2) radiation from apertures into adjacent apertures. Study of a previously investigated three-room geometry indicates that this phenomenon can notably affect the shape of decay curves in subrooms.

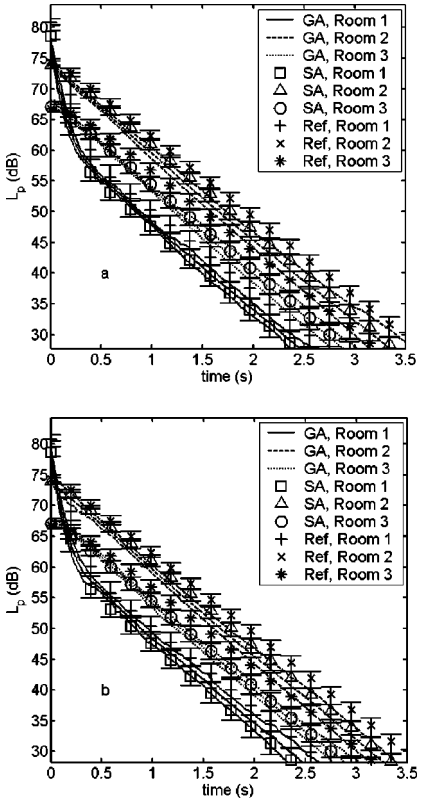

FIG. 9. For the three-room coupled system (Fig. 1), the GA model (ensemble averages of all receiver positions within each of the subrooms) (GA) is compared with the improved SA model [Eq. (11), $\eta = \alpha''/\overline{\alpha}$] (SA) and Kuttruff's original SA model [Eq. (11), $\eta = 1$] (Ref) for two different scattering coefficients $s = 0.40$ (a) and 0.99 (b). In the improved model the correction for nondiffuse transmission between the subrooms is used but the solid-angle correction for the initial power distribution is not. For each GA curve the lines on either side of the central curve represent the region of confidence defined by u_i, assuming α and s are known to $\pm 10\%$ at the same level of confidence. Error bars represent the regions of confidence for SA and reference curves assuming α is known to $\pm 10\%$ at the same level of confidence.

Uncertainty in the values of input parameters to the models (α and s) has a greater effect on predictions of the SA model than those of the GA model, such that GA and SA predictions can often be considered equivalent. For the $\pm 10\%$ input uncertainty used here, the resulting uncertainties in the predictions are large enough to obscure differences between different SA decay models. They are also large enough to be audibly significant, indicating the particular importance of accurate input parameters for modeling coupled rooms.[35]

B. Recommendations

Though developing a SA model that is consistently accurate in all circumstances is difficult, for many cases, the model presented here should prove applicable at high frequencies. Geometrical acoustics is an intrinsically high-frequency model and therefore can only assess the accuracy of the SA model in the limit of vanishing wavelength. However, in practice, the frequency range of validity can extend into the 1000 Hz octave band or below.[35] At lower frequencies, other methods, such as those described in Ref. 35, should be used.

ACKNOWLEDGMENTS

This work was supported by the Bass Foundation and the Rensselaer Polytechnic Institute School of Architecture. J.E.S. gratefully acknowledges B.-I. L. Dalenbäck, for development of a new algorithm in CATT-Acoustic, and N. Xiang, for discussions concerning Bayesian parameter estimation.

[1] W. B. Joyce, ''Sabine's reverberation time and ergodic auditoriums,'' J. Acoust. Soc. Am. **58**, 643–655 (1975).
[2] E. N. Gilbert, ''Ray statistics in reverberation,'' J. Acoust. Soc. Am. **83**, 1804–1808 (1988).
[3] J. D. Polack, ''Modifying chambers to play billiards: the foundations of reverberation theory,'' Acustica **76**, 257–272 (1992).
[4] H. Kuttruff, ''Simulierte Nachhallkurven in rechteckräumen mit diffuseen schallfeld,'' (''Simulated decay curves in rectangular rooms with diffuse sound fields'') Acustica **25**, 333–342 (1971).
[5] O. Legrand and D. Sornette, ''Test of Sabine's reverberation time in ergodic auditoriums within geometrical acoustics,'' J. Acoust. Soc. Am. **88**, 865–870 (1990).
[6] F. Mortessange, O. Legrand, and D. Sornette, ''Role of the absorption distribution and generalization of exponential reverberation law in chaotic rooms,'' J. Acoust. Soc. Am. **94**, 154–161 (1993).
[7] M. Hodgson, ''Evidence of diffuse surface reflection in rooms,'' J. Acoust. Soc. Am. **89**, 765–771 (1991).
[8] W. C. Sabine, *Collected Papers on Acoustics* (Dover, New York, 1964); see also W. S. Franklin, ''Derivation of equation of decaying sound in a room and definition of open window equivalent of absorption power,'' Phys. Rev. **16**, 372–374 (1903); G. Jäger, ''Zur theorie des nachhalls,'' (''On the theory of reverberation'') Sitzungsber. Akad. Wiss. Wien, Math.-Naturwiss. Kl., Abt. 2A **120**, 613–634 (1911).
[9] K. Schuster and W. Waetzmann, ''Nachhall in geschlossenen Räumen,'' (''Reverberation in closed rooms'') Ann. Phys. (Leipzig) **1**, 671–695 (1929); R. F. Norris, ''An instrumental method of reverberation measurement,'' presented at the 1st meeting of the Acoustical Society of America, New York, 10–11 May 1929, published in Ref. 23 Appendix II, pp. 603–605; C. F. Eyring, ''Reverberation time in 'dead' rooms,'' J. Acoust. Soc. Am. **1**, 217–241 (1930).
[10] G. Millington, ''A modified formula for reverberation,'' J. Acoust. Soc. Am. **4**, 69–82 (1932); W. J. Sette, ''A new reverberation time formula,'' *ibid.* **4**, 193–210 (1932).
[11] H. Kuttruff, ''Weglängverteilung und Nachhallverlauf in Räumen mit diffuse reflektierenden Wänden,'' (''Path-length distributions and reverberation processes in rooms with diffusely reflecting walls'') Acustica **23**, 238–239(L) (1970); see also Ref. 17 pp. 122–126.
[12] T. M. W. Embleton, ''Absorption coefficients of surfaces calculated from decaying sound fields,'' J. Acoust. Soc. Am. **50**, 801–811 (1971); see also A. D. Pierce, *Acoustics: An Introduction to Its Physical Principles and Applications* (Mc–Graw Hill, New York, 1981), pp. 265–267.
[13] A. H. Davis, ''Reverberation equations for two adjacent rooms connected by an incompletely sound-proof partition,'' Philos. Mag. **50**, 75–80 (1925).
[14] L. Cremer and H. A. Müller, *Principles and Applications of Room Acoustics*, trans. T. J. Schultz (Applied Science, New York, 1982), Vol. 1, pp. 261–283.
[15] C. D. Lyle, ''The prediction of steady state sound levels in naturally coupled enclosures,'' Acoust. Lett. **5**, 16–21 (1981).
[16] C. D. Lyle, ''Recommendation for estimating reverberation time in coupled spaces,'' Acoust. Lett. **5**, 35–38 (1981).
[17] H. Kuttruff, *Room Acoustics*, 4th ed. (Spon, New York, 2000), pp. 110–114, 126–129, 130, 133–137, 139–141, 142–145.
[18] V. M. A. Peutz, ''Electrical analog for studying acoustical coupled rooms,'' Fifth International Congress on Acoustics, Liége, Belgium, 7–14, Sept. 1965, paper G34.
[19] C. F. Eyring, ''Reverberation time measurement in coupled rooms,'' J. Acoust. Soc. Am. **3**, 181–206 (1931).
[20] W. B. Joyce, ''Power series for the reverberation time,'' J. Acoust. Soc. Am. **67**, 564–571 (1980).
[21] H. Kuttruff and Th. Straßen, ''Zur Abhängigkeit des Raumnachhalls von der Wanddiffusität und von der Raumform'' (''On the dependence of reverberation time on the 'wall diffusion' and on room shape''), Acustica **45**, 246–255 (1980).
[22] M. Hodgson, ''When is diffuse-field theory accurate?'' in Proc. Wallace Clement Sabine Centennial Symposium, Cambridge, MA, 1994, pp. 157–160 [also on the CD-ROM: *Proceedings of the Sabine Centennial Symposium on CD ROM* (available from the Acoustical Society of America), paper 1pAAe2].
[23] V. O. Knudsen, *Architectural Acoustics* (Wiley, New York, 1932) pp. 130–132, 141–143.
[24] M. Vorländer, ''Revised relation between the sound power and the average sound pressure level in rooms and consequence for acoustics measurements,'' Acustica **81**, 332–343 (1995).
[25] R. N. Miles, ''Sound field in a rectangular enclosure with diffusely reflecting boundaries,'' J. Sound Vib. **92**, 203–226 (1984).
[26] M. Barron and L.-J. Lee, ''Energy relations in concert auditoriums I,'' J. Acoust. Soc. Am. **84**, 618–628 (1988).
[27] M. Vorländer, ''Room acoustical simulation algorithm based on the free path distribution,'' J. Sound Vib. **232**, 129–137 (2000).
[28] P. W. Smith, Jr., ''Statistical models of coupled dynamical systems and the transition from weak to strong coupling,'' J. Acoust. Soc. Am. **65**, 695–698 (1979).
[29] W. B. Joyce, ''The exact effect of surface roughness on the reverberation time of a uniformly absorbing spherical enclosure,'' J. Acoust. Soc. Am. **64**, 1429–1436 (1978).
[30] A. Le Bot and A. Bocquillet, ''Comparison of an integral equation on energy and the ray-tracing technique in room acoustics,'' J. Acoust. Soc. Am. **108**, 1732–1740 (2000).
[31] B.-I. L. Dalenbäck, ''Room acoustic prediction based on a unified treatment of diffuse and specular reflection,'' J. Acoust. Soc. Am. **100**, 899–909 (1996).
[32] B.-I. L. Dalenbäck, ''Verification of prediction based on Randomized Tail-Corrected cone-tracing and array modeling,'' on the CD-ROM: *Collected Papers, 137th Meeting of the Acoustical Society of America and the Second Convention of the European Acoustical Association*, Berlin, 14–19 March 1999 (ISBN) 3-9804458-5-4, available from Deutsche Gesellschaft für Akustik, Fachbereich Physik, Universität Oldenburg, 26111 Oldenburg, Germany), paper 3pAAa1. [J. Acoust. Soc. Am. **105**, 1173(A) (1999)].
[33] H. Kuttruff, ''Zum Einfluß eines winkelabhängigen Schallabsorptionsgrades auf die Nachhallzeit'' (''On the influence of an angle-dependent sound absorption coefficient on reverberation time''), Acustica **42**, 187–188(L) (1979).
[34] G. Benedetto and R. Spagnolo, ''Reverberation time in enclosures: The surface reflection law and the dependence of absorption coefficient on the angle of incidence,'' J. Acoust. Soc. Am. **77**, 1447–1451 (1985).
[35] J. E. Summers, *Reverberant acoustic energy in auditoria that comprise systems of coupled rooms* (Ph.D. dissertation, Rensselaer Polytechnic Institute, Troy, NY, 2003).
[36] F. Kawakami and K. Yamaguchi, ''Space-ensemble average of reverberation decay curves,'' J. Acoust. Soc. Am. **70**, 1071–1082 (1981).
[37] ISO 3382, ''Acoustics—Measurement of the reverberation time of rooms with reference to other parameters,'' 1997.
[38] J. Giner, C. Militello, and A. García, ''Ascertaining confidence within the ray-tracing method,'' J. Acoust. Soc. Am. **106**, 816–823 (1999); ''The Monte Carlo method to determine the error in calculation of objective acoustic parameters within the ray tracing technique,'' *ibid.* **110**, 3081–3085 (2001).
[39] P. R. Bevington and D. K. Robinson, *Data Reduction and Error Analysis for the Physical Sciences*, 2nd ed. (McGraw–Hill, New York, 1992), pp. 41–50.
[40] S. G. Rabinovich, *Measurement Errors and Uncertainties: Theory and Practice*, 2nd ed., trans. M. E. Alferieff (Springer, New York, 2000), pp. 166–172.